

Direct observation of antiphase domains in $\text{Bi}_2\text{Sr}_2\text{CaCu}_2\text{O}_8$ by transmission electron microscopy

This article has been downloaded from IOPscience. Please scroll down to see the full text article.

1989 J. Phys.: Condens. Matter 1 317

(<http://iopscience.iop.org/0953-8984/1/1/028>)

View [the table of contents for this issue](#), or go to the [journal homepage](#) for more

Download details:

IP Address: 171.66.16.89

The article was downloaded on 10/05/2010 at 15:53

Please note that [terms and conditions apply](#).

LETTER TO THE EDITOR

Direct observation of antiphase domains in $\text{Bi}_2\text{Sr}_2\text{CaCu}_2\text{O}_8$ by transmission electron microscopy

K K Fung^{†‡}, R L Withers^{†§}, Y F Yan[‡] and Z X Zhao[‡]

[†] Beijing Laboratory of Electron Microscopy, Chinese Academy of Sciences, 100080 Beijing, People's Republic of China

[‡] Institute of Physics, Chinese Academy of Sciences, 100080 Beijing, People's Republic of China

[§] Research School of Chemistry, Australian National University, Canberra, ACT, Australia

Received 24 October 1988

Abstract. Antiphase domains associated with a commensurate modulation in $\text{Bi}_2\text{Sr}_2\text{CaCu}_2\text{O}_8$ have been directly observed by transmission electron microscopy. A model of the antiphase boundary based on group theoretical considerations is put forward to explain the non-conservative nature of the antiphase boundary. It is suggested that the presence of antiphase domains may have important implications for the superconducting critical current of this compound.

Recently, new high-temperature superconducting oxides have been discovered in the Bi–Sr–Ca–Cu–O and Tl–Ba–Ca–Cu–O systems (Michel *et al* 1987, Maeda *et al* 1988, Sheng and Hermann 1988). Both the Bi-based and Tl-based oxides are closely related to the Aurivillius phases (Aurivillius 1949). They can be described as slabs of perovskite-related layers sandwiched between double Bi or Tl oxide layers. The underlying perovskite-related structure is evident in the Tl-based oxides and the crystal structure is tetragonal with space group $I4/mmm$ (Subramanian *et al* 1988a). The tetragonal structure is also weakly modulated incommensurately (Liu *et al* 1988). In the case of the Bi-based oxides, the underlying perovskite-related structure is obscured by a strong incommensurate modulation as well as a $\frac{1}{2}(110)_p^*$ commensurate modulation, where the subscript p refers to the perovskite-related structure. This results in an expanded $\sqrt{2}a_p \times \sqrt{2}a_p$ basal plane cell for the average structure. The average crystal structure is now orthorhombic with space group $Amaa$ (Subramanian *et al* 1988b, Withers *et al* 1988a). Note that the basal plane components of the weak incommensurate modulations in the Tl-based superconducting phases point along the perovskite axes while it is along an axis at 45° to the perovskite axes in the case of the Bi-based oxides. The modulations in $\text{Bi}_2\text{Sr}_2\text{CaCu}_2\text{O}_8$ have been studied by transmission electron microscopy (TEM). We report in this Letter the direct observation of antiphase domains associated with the commensurate modulation.

Single crystals of $\text{Bi}_2\text{Sr}_2\text{CaCu}_2\text{O}_8$ grown by the flux method were obtained in the form of platelets. The superconducting temperature is 93 K (Yan *et al* 1988). Specimens

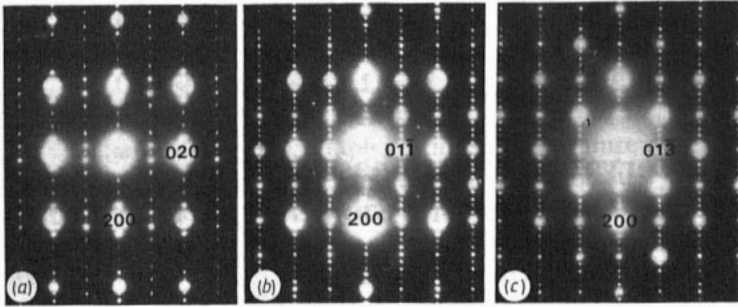


Figure 1. Selected area electron diffraction patterns from (a) [001], (b) [011] and (c) [013] zone axes of $\text{Bi}_2\text{Sr}_2\text{CaCu}_2\text{O}_8$. The [011] and [013] patterns were obtained from [001] by tilting about the a^* axis.

for TEM were prepared by repeated cleavage along the basal plane. Figure 1(a) shows an [001] diffraction pattern of $\text{Bi}_2\text{Sr}_2\text{CaCu}_2\text{O}_8$. The orthorhombic axes and the perovskite axes are shown as marked. Figure 1(b) and (c) are obtained from figure 1(a) by tilting about the orthorhombic a^* axis. Note the $0k0$ reflections for odd values of k are



Figure 2. Imaging of the antiphase domains in $\text{Bi}_2\text{Sr}_2\text{CaCu}_2\text{O}_8$. (a) bright-field imaged with a basic reflection (020), (b) and (c) bright-field and dark-field imaged with a superlattice reflection ($01\bar{1}$). The curved band down the centres of the images is a group of four dislocation ribbons.

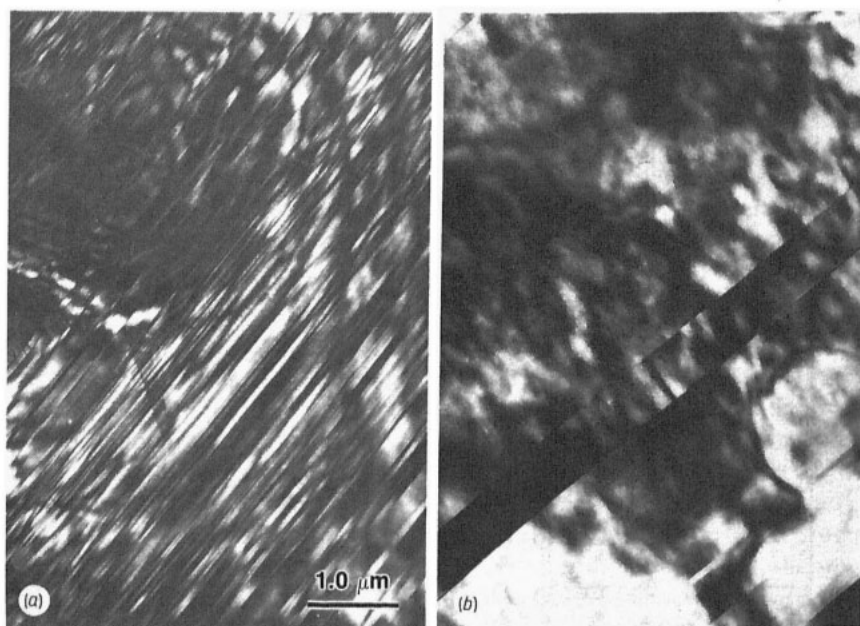


Figure 3. The density of antiphase domains is sometimes rather high (*a*), but it is usually much lower (*b*). Patches of the same contrast in (*b*) arise from an incommensurate reflection. Note how the contrast stops abruptly at an antiphase boundary.

absent (figure 1(*a*)). However, the $01\bar{1}$ and $01\bar{3}$ reflections can be excited when tilted away from the $[001]$ axis (figure 1(*b*) and (*c*)). The $01\bar{1}$ or $01\bar{3}$ reflections are in fact quite intense so that dark-field patterns can readily be taken. An $01\bar{1}$ dark-field image is shown in figure 2. The corresponding bright-field image and a 020 bright-field image taken when the $01\bar{1}$ reflection is not excited is also shown in figure 2. The images are actually taken with the crystal tilted off the zone axes about $[01\bar{1}]^*$ so that a systematic row is obtained. It is clear that dark and bright bands are only visible in bright and dark field when the $01\bar{1}$ reflection is excited. The 020 bright-field image shows no traces of the bands. Note how the dark and bright bands alternate along the bend contour. The contrast of a given band also reverses on crossing the bend contour. The inset in figure 2 shows clearly that the bands are oriented perpendicular to the a^* axis. These bands are also visible when imaged with the $01\bar{3}$ reflection near the $[031]$ zone axis. In fact, when the crystal is tilted from the $[031]$ zone axis through the $[011]$, $[001]$, $[0\bar{1}1]$ to the $[0\bar{3}1]$ zone axis, the bands are visible whenever the $01\bar{3}$, $01\bar{1}$, 011 and 013 reflections are excited. The angle from $[031]$ to $[0\bar{3}1]$ spans some 55° . We infer that the bands are domains separated by planar boundaries parallel to the 100 planes. It is also found that the density of the bands and their separation vary over a wide range. This is shown in figure 3. The domains in figure 3(*a*) are closely and more or less evenly spaced, with an averaged width of about 30 nm. Domains larger than a few μm are visible in figure 3(*b*), but small domains are also visible. $[001]$ convergent beam electron diffraction (CBED) (Steeds 1979) patterns taken from adjacent domains are identical. Tanaka patterns (Tanaka *et al* 1980) taken from a region containing several domains do not show any sign of change across the domain boundaries. The boundaries are therefore coherent planes.

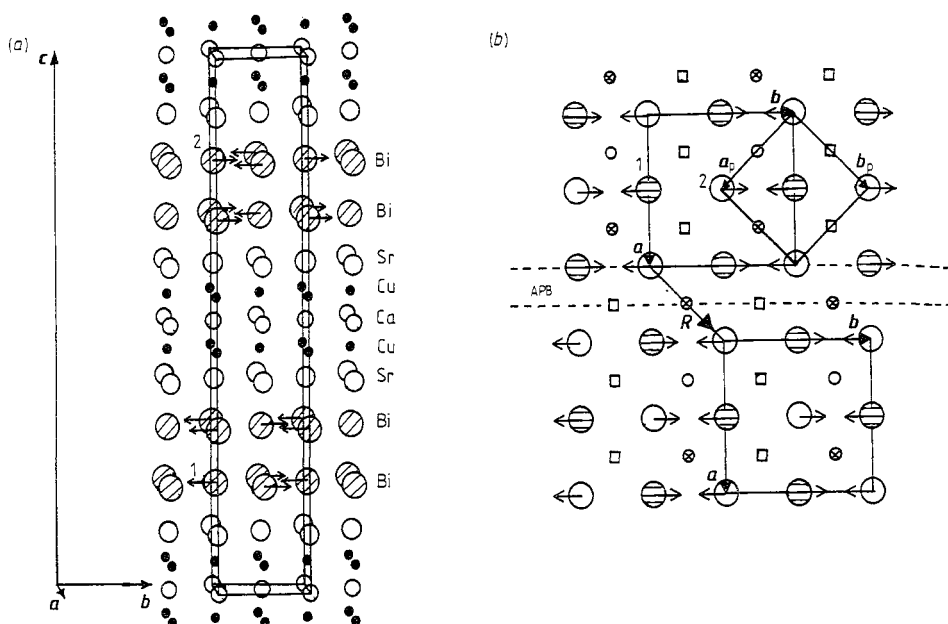


Figure 4. (a) Locations of metal atoms in the unit cell of $\text{Bi}_2\text{Sr}_2\text{CaCu}_2\text{O}_8$. (b) Basal plan view of the lower double Bi layers and oxygen between the Bi layers. The arrows on the Bi atoms indicate the shifts along the b axis. Oxygen vacancies are indicated by open squares, oxygen atoms by small circles. The upward and downward shift of the oxygen atoms are denoted by open and crossed circles. The displacement vector is $\frac{1}{2}[110]$. Note how the atoms are shifted across the antiphase boundary (APB).

This suggests that the domains are antiphase domains. In addition to the CBED evidence, twins can also be ruled out since no split spots have been seen in the diffraction patterns. The point group deduced from the CBED patterns is mmm (Zhang *et al* 1988), in agreement with the result obtained by Subramanian *et al* (1988b) and Withers *et al* (1988a). Treating the $Amaa$ orthorhombic cell as a superlattice cell of the $I4/mmm$ tetragonal cell, we see that the translations $\frac{1}{2}[110]$, $\frac{1}{2}[101]$ which are Bravais lattice vectors in the tetragonal cell are no longer lattice vectors with respect to the orthorhombic cell. These vectors are obvious choices for the displacement vector (R) of the antiphase domains (Amelinckx and van Landuyt 1978). Indeed, for this choice of R and $q = 011$ or 013 , $2\pi q \cdot R = \pi$. Note that the displacement vector $\frac{1}{2}[110]$ is in the basal plane and $\frac{1}{2}[101]$ is obtained by adding a Bravais lattice vector of the A -centred orthorhombic cell, i.e. $\frac{1}{2}[0\bar{1}1]$, to $\frac{1}{2}[110]$ (figure 4). Note that $\frac{1}{2}[110]$ is not parallel to the antiphase boundary. Therefore the antiphase boundary is non-conservative.

In a group theoretical study of the Bi-based superconducting oxides and the related Aurivillius phases, Withers *et al* (1988a, b) proposed that the enlarged $\sqrt{2}a_p \times \sqrt{2}a_p$ orthorhombic basal-plane cell is related to the tetragonal perovskite-related cell by a $\frac{1}{2}(110)_p^*$ modulation characterised by a specific irreducible representation (R_2). Such an irreducible representation severely constrains the form of any associated compositional or displacive ordering. In the case of the displacive component of the modulation, all metal atom shifts must be along the b -axis. They have also shown that any associated compositional ordering can only be associated with the oxygen sites in square planar

configuration around the Cu atoms or the oxygen sites midway between the Bi layers. The structural refinement of Kajitani *et al* (1988) suggests that the two oxygen sites midway between the Bi layers are, on average, approximately 50% occupied. Using this result, they deduced that any compositional ordering must be due to alternating strings of occupied and unoccupied oxygen atom sites. The associated displacement of the corresponding atoms obtained from group theoretical consideration are as follows: the oxygen atoms are shifted along the c axis normal to the basal plane whereas the Bi atoms are shifted along the b axis in the basal plane. The results reported by Subramanian *et al* (1988b) support this prediction. The Bi atoms are found to show the largest distortion amplitude while the Cu atoms are virtually undisturbed. This makes sense since the presence of oxygen vacancies midway between the Bi layers allows the Bi atoms to relax. The Bi bilayers in the unit cell and the ordering of oxygen vacancies between the Bi layers and the shift of the Bi atoms and oxygen atoms in projection are shown schematically in figure 4. The displacement vector $\frac{1}{2}[110]$ shifts an unoccupied oxygen site to an occupied site on the same side of the antiphase boundary, but across the boundary, it shifts empty site to empty site, occupied up (down) site to occupied up (down) site. Consequently, strings of oxygen vacancies are shifted to align with strings of occupied oxygen atoms across the boundary and vice versa. For the Bi atoms, consider the upper layer, the shift in the b direction is parallel to the boundary. On the same side of the boundary, adjacent rows of Bi atoms are shifted in the opposite sense. Across the boundary, two adjacent rows of Bi atoms are shifted in the same sense. The Bi atoms in the lower layer which are located in projection in the centre of the upper layer atoms are similarly shifted. Normal to the boundary, Bi atoms of the same sense of shift are lined up parallel to the strings of oxygen atoms. Across an antiphase boundary, the Bi atoms are shifted in the opposite sense. The non-conservative antiphase boundary can therefore be regarded as due to the removal of one row of Bi atoms and one row of oxygen vacancies and oxygen atoms at up sites.

So far, we treated the commensurate modulation and the incommensurate modulation in $\text{Bi}_2\text{Sr}_2\text{CaCu}_2\text{O}_8$ as being independent. The incommensurate modulation is characterised by a wavevector $q = 0.21a^* + c^*$. An incommensurate satellite appears as a zigzag contour in a bent specimen while a basic reflection appears as a smooth contour in a diffraction contrast image. By exciting an incommensurate satellite reflection in a flat region, a mottled contrast associated with the incommensurate modulation can be observed in the dark field and the bright field. By simultaneously exciting both an incommensurate satellite and the $01\bar{1}$ reflection, both the contrast caused by the incommensurate reflection and the antiphase domains are clearly visible. Such an image is shown in figure 3(b). Patches of similar contrast caused by the incommensurate reflection are of irregular shape elongated along the a direction. It can be seen that patches of the same contrast stop abruptly at an antiphase boundary. This means that the assumption that the incommensurate and commensurate modulations are independent is not true. In view of the fact that the antiphase boundary acts as a barrier to these incommensurate patches, it is expected that it may also affect the transport properties of the superconductor. The boundaries can function as pinning sites. Since the density of the antiphase domains varies by several orders of magnitude, their effect should be detectable. The variation of the density of antiphase domain boundaries is probably caused by different growth conditions and cooling rates. Since the antiphase boundaries are parallel to the a planes, the transport properties of high-density domain samples should show planar anisotropic effects in the a and b directions. We speculate that the superconducting critical current might be dependent on the density of antiphase

domains. If this is the case, the critical current might be controllable by varying the density of antiphase domains. This awaits experimental confirmation.

The work reported here was supported in part by the National Center for Research and Development on Superconductivity. RLW visited China on an exchange programme between the Australian Academy of Science and the Chinese Academy of Sciences.

References

- Amelinckx S and Van Landuyt J 1978 *Diffraction and Imaging Techniques in Materials Science* ed. Amelinckx, Gevers and Van Landuyt (Amsterdam: North-Holland) p 107
- Aurivillius B 1949 *Ark. Kemi* **1** 463, 499
- Kajitani T, Kusaba K, Kikuchi M, Kobayashi N, Syono Y, Williams T B and Hirabayashi M 1988 *Japan. J. Appl. Phys.* **27** 587
- Liu Y, Zhang Y L, Liang J K and Fung K K 1988 *J. Phys. C: Solid State Phys.* **21** 1039
- Maeda H, Tanaka Y, Fukutomi M and Asano T 1988 *Japan. J. Appl. Phys.* **27** L209
- Michel C, Hervieu M, Borel M M, Grandin A, Deslandes F, Provost J and Raveau B 1988 *Z. Phys. B* **68** 421
- Sheng Z Z and Hermann A M 1988 *Nature* **332** 55, 138
- Steeds J W 1979 *Introduction to Analytical Electron Microscopy* ed. Hren, Goldstein and Joy (New York: Plenum) p 387
- Subramanian M A, Calabrese J C, Torardi C C, Gopalakrishnan J, Askew T R, Flippen R B, Morrissey K J, Chowdhry U and Sleight A W 1988b *Science* **239** 1015
- Subramanian M A, Torardi C C, Calabrese J C, Gopalakrishnan J, Morrissey K J, Askew T R, Flippen R B, Chowdhry U, Sleight A W 1988b *Science* **239** 1015
- Tanaka M, Saito R, Ueno K and Harada Y 1980 *J. Electron Microsc.* **29** 408
- Withers R L, Anderson J S, Hyde B G, Thompson J G, Wallenberg L R, FitzGerald J D and Stewart A M 1988a *J. Phys. C: Solid State Phys.* **21** L417
- Withers R L, Thompson J G, Wallenberg L R, FitzGerald J D, Anderson J S and Hyde B G 1988b *J. Phys. C: Solid State Phys.* **21** 6067
- Yan Y F, Li C Z, Wang J H, Chang Y C, Yang Q S, Hou D S, Chu X, Mai Z H, Zhang H Y, Zheng D H, Ni Y M, Jia S L, Shen D H and Zhao Z X 1988 *Mod. Phys. Lett. B* **2** 571
- Zhang X F, Yan Y F and Fung K K 1988 *J. Chinese Electron Microsc. Soc.* **7** 154 (in Chinese)